Microscopy analysis of the morphology and phase transformation of metastable β-HgI$_2$

XU GANG[a,*], CHEN JING[a], GU ZHI[b], HOU YANNAN[a], LI JUNYING[a], YANG CONGXIAO[a]

[a]School of Materials and Chemical Engineering, Xi'an Technological University, Xi'an, 710032, Shaan Xi Province, P. R. China
[b]State Key Laboratory of Solidification Processing, North western Polytechnical University, Xi'an, 710072, Shaan Xi Province, P. R. China

Rhombus-shaped metastable β-HgI$_2$ crystals were grown in a mixture of dimethylsulfoxide and H$_2$O at constant temperature. Crystal growth and phase transformation (β-HgI$_2 \rightarrow \alpha$-HgI$_2$) were investigated *in situ* using polarizing microscopy. The attachment energy of the main faces of β-HgI$_2$ crystals was calculated to investigate crystal morphology. The results showed that the newly-grown crystal belong to $Cmc2_1$ space group, and the included angle of (110) and $(1\bar{1}0)$ planes during crystal growth remains approximately 65.24°, in accordance with that in unit cell of β-HgI$_2$(65.16°). The morphological importance decreases differently as {001} >{110} >{111} >{112} >{010}, indicating a rhombus layer shape under the employed condition. For the β-HgI$_2 \rightarrow \alpha$-HgI$_2$ phase transformation, we fitted the relation between the transformed volume fraction *f*, and time *t*, and obtained a growth exponent of *n* = 1.5, suggesting the growth mode is between one-dimensional and two-dimensional growth. Comparison of the parent and product structures indicates that the metastable β-HgI$_2 \rightarrow \alpha$-HgI$_2$ phase transformation follows a first-order structural reconstruction.

(Received June 27, 2018; accepted April 8, 2019)

Keywords: Mercuric iodide, Crystal structure, Growth Morphology, Phase transformation

1. Introduction

Mercuric iodide (HgI$_2$) is a promising material for X-ray detectors due to its high sensitivity and resolution [1]. It is also a novel photocatalyst for treating environmental pollution [2]. Crystalline HgI$_2$ has great potential as a direct photoconducting converter for digital X-ray imaging because it exhibits the highest X-ray sensitivity among known polycrystalline materials [1]. The growth of bulk HgI$_2$ crystals in solution has been studied for several decades [3-7]. The structure of the HgI$_4^{2-}$ complex in solutions of mercuric iodide in dimethylsulfoxide (DMSO) was found to be consistent with values from tetrahedral HgI$_4^{2-}$ crystal structures [8]. DMSO was also found to be an effective solvent for the growth of large mercuric iodide crystals in solution [9]. Detector-level HgI$_2$ single crystals have been prepared, and the energy resolution of the resulting detector measured [4,9]. Nicolau reported the crystallisation of α-HgI$_2$ from iodomercurate complexes, investigated the mechanisms of the formation of the octahedron and prism faces [10], and obtained characteristic of γ-ray detection spectra [11].

Polycrystalline HgI$_2$ film has emerged as an interesting alternative to bulk crystals over the past 15-20 years [12-16] following the development of large area X-ray radiation and digital radiographic detectors for medical diagnostic applications. In particular, films with the thickness of 150μm are sufficient for capturing 99% of

radiation for 50keV energy [17]. For polycrystalline materials, charge transport along the *c*-axis of microcrystals is dependent on the orientation of crystal. Furthermore, the resistivity of oriented films is two orders of magnitude higher than that of poly-films [18]. Noguera et al. suggested that the main challenge of the development of direct X-ray imagers made from HgI$_2$ is the requirement to grow highly oriented films [18]. To this end, much research aimed at obtaining the preferred orientation has been conducted [19-22].

Recently, Fornaro et al. investigated the control of the morphology and size of mercuric iodide, and focused on nanostructure and nucleation of heavy metal iodides [23, 24]. Their study showed that using nanostructures as precursors for growing epitaxial layers is a promising method for obtaining the preferred orientation of polycrystalline mercuric iodide [25]. However, mercuric iodide is known to crystallise both in solution [26] and from vapor [27] into three concomitant polymorphs coloured red, orange, and yellow [28]. Jovan et al. reported that the yellow crystal (metastable β-HgI$_2$) is formed during the initial phase of crystal growth [6]. Meanwhile, others [29] reported that the formation of microcrystals of stable α-HgI$_2$ is preceded by the formation and growth of particles of the metastable yellow and orange forms. However, metastable β-HgI$_2$ is known to be mechanically unstable [26]; when the conditions change, the metastable β-HgI$_2 \rightarrow \alpha$-HgI$_2$ phase transform can occur. The metastable β-HgI$_2$ has orthorhombic $Cmc2_1$

symmetry, while α-HgI$_2$ has P4$_2$$nmc$ symmetry. The metastable β-HgI$_2$$\rightarrow$$\alpha$-HgI$_2$ phase transformation affects the orientation of the nucleation and growth of α-HgI$_2$, and is structure destructive. Hence, it is necessary to study the crystal structure and phase transformation of β-HgI$_2$ to better understand the mechanism of formation of the more preferred orientation of α-HgI$_2$.

2. Experimental

Faster evaporation favours the formation of metastable β-HgI$_2$ [28], and metastable β-HgI$_2$ is formed during the initial phase of crystal growth. Hence, acquiring the metastable β-HgI$_2$ by solvent evaporation is convenient. α-HgI$_2$ powder with a nominal purity of 99.9% was selected as the starting material for growing crystals from the DMSO (C$_2$H$_6$OS) and H$_2$O solvent mixture. α-HgI$_2$ salt (0.02g) was added to 8ml of DMSO in a 50ml beaker with constant agitation for 10 min at 35°C and a colourless solution was formed. Indium tin oxide (ITO) glass (10×10×1mm^3) was placed in the beaker, and 20ml of deionised H$_2$O was slowly added at a rate of 1 drop per s to form the 1:2.5 DMSO:H$_2$O (v/v) solution. The beaker was incubated in the dark at 35°C for 20h. The ITO glass was then removed and placed on the objective table of the microscope. Due to the rapid decrease in temperature, the growth and/or phase change of crystals could be observed within 10 min, along with the volatilisation of DMSO and H$_2$O.

Growth processes and morphology changes of metastable β-HgI$_2$ were recorded at room temperature using a LEICA DM 2500P polarizing microscope (Wetzlar, Germany). The structure of the newly-grown crystal was characterised at room temperature using SHIMADZU 6000 X-ray diffraction apparatus, with Cu-K$_\alpha$ radiation (λ=1.54056 Å) in the 2θ range between 10° to 80° in steps of 0.02°. The attachment energy of the crystallographic plane and the area of the crystal were calculated using Material Studio software and Image J processing software, respectively. The crystal structure was drawn using DIAMOND 3.0.

3. Results and discussion

The growth of metastable β-HgI$_2$ crystals was recorded using successive images captured on a LEICA DM2500P polarising microscope. The total recording time was 105s and images were captured in 15 s, as shown in Fig. 1. The two edges (A and B) expanded uniformly at an average rate of 0.71 μm/s, and the average included angle of A and B was ~65.24° during the entire growth process. Since specimens contained some solution, faster solvent evaporation lead to the growth of yellow HgI$_2$ (metastable β-HgI$_2$) crystals, and growth stopped when all solvent had volatilised.

The standard structure of metastable β-HgI$_2$ is shown in Fig. 2(a) and was plotted using DIAMOND 3.0 based on data derived from the orthorhombic structure of HgI$_2$ (JCPDF card 73-0456). The results of the simulation indicate that metastable β-HgI$_2$ is a classical molecular crystal, with almost linear I-Hg-I molecules packed by Van der Waals forces, implying an unstable structure [24].
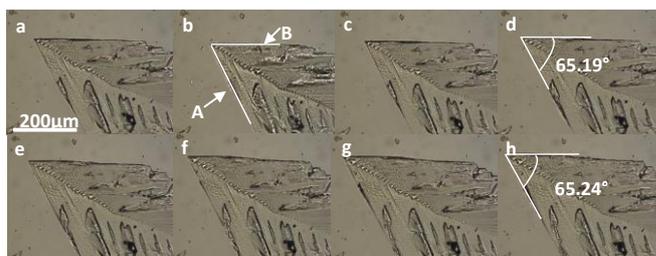

Fig. 1. Optical images of the growth of metastable β-HgI$_2$ crystal
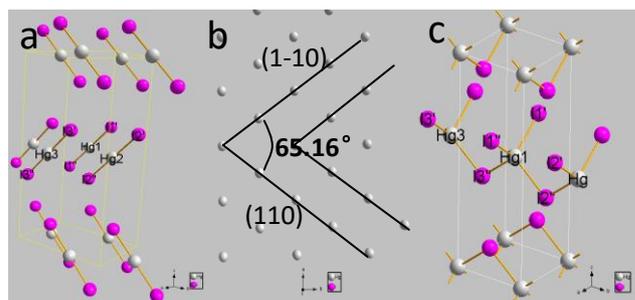

Fig. 2. Structure of HgI$_2$. (a) Unit cell of metastable β-HgI$_2$ (b) Hg packing of the (001) face of β-HgI$_2$ (c) Structure of α-HgI$_2$

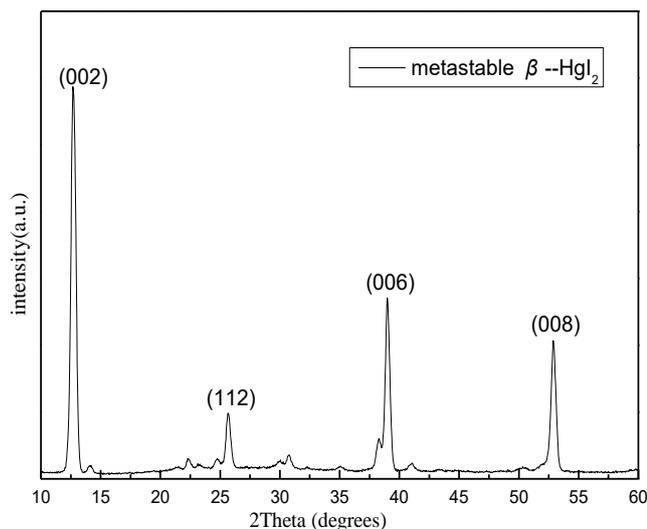*Fig. 3. Photo showing the metastable β-HgI$_2$ crystal morphology*

Fig. 4. XRD pattern of metastable β-HgI$_2$

To further investigate the characteristics of the growth interface, the packing of HgI$_2$ molecules (atomic Hg) from the c-axis direction was investigated in Fig. 2(b). The separation angle between (110) and ($1\bar{1}0$) faces was calculated to be 65.16°, consistent with that of the A and B edge shown in Fig. 1, suggesting A and B are (110) and ($1\bar{1}0$), respectively. The habit (external morphology) of a crystal is controlled by both the external (environmental) conditions of crystallisation and the internal (structural) factors present in the crystal. Thus, the stable included angle (reflecting the internal factors) suggests that crystal growth continued close to equilibrium. The structure of α-HgI$_2$ is shown in Fig. 2(c), and the difference between β-HgI$_2$ and α-HgI$_2$ are discussed below.

The newly-grown crystals are shown in Fig. 3. Most are colourless and rhomboid, and the largest face is shown in vertical orientation. All acute angles in the colourless rhomboid crystals are ~65.0 ± 0.35°. The structure of metastable β-HgI$_2$ was investigated by XRD (Fig. 4). Peaks corresponding to (002), (112), (006) and (008) appeared at 10°-60°. The structural symmetries could be indexed well using the orthorhombic structure of HgI$_2$ (JCPDF card73-0456). The intensity of the (001) peak in the XRD pattern shows the main crystal face in Fig. 3. To further understand the contours of metastable β-HgI$_2$ in Fig. 3, the attachment energy of the main faces was investigated by Periodic Bond Chain theory (PBC) in which only strong bonds are defined as bonds in the first coordination sphere, and the attachment energy is defined as the energy released per mole when a new layer is deposited on a crystal face [30]. Thus, the attachment energy of the main plane of the orthorhombic structure of metastable β-HgI$_2$ was calculated to investigate the morphological importance based on the Attachment Energy (AE) Matrix in Morphology module in Material Studio (MS) software.

The growth rate of crystal facet R_{hkl} was found to be in proportion with the attachment energy E_{hkl}^{att} [31, 32]. As shown in Eq. (1),

$$R_{hkl} \propto E_{hkl}^{att} \tag{1}$$

and E_{hkl}^{att} can be derived from Eq. (2)

$$E_{hkl}^{att} = E^{cr} - E_{hkl}^{slice} \tag{2}$$

where, E^{cr} is the crystal lattice energy, E_{hkl}^{slice} is the two-dimensional lattice energy on the growing face, and E_{hkl}^{att} is the energy released when the growth unit attaches to the interface of the crystal. The lower the attachment energy, the slower the growth rate of the facet. The attachment energy (J/mol) of the main face of metastable β-HgI$_2$ was calculated and is listed in Table 1.

The attachment energy was calculated to be 7.5 J/mol for the (001) plane of metastable β-HgI$_2$, and this was the lowest value among the five common faces (Table 1). Thus, the important morphological face of metastable β-HgI$_2$ is (001), consistent with the results of the XRD experiments. Plane (110) is inferior one compared with (001) based on the attachment energy of 18.4 J/mol. Given the unit cell shown in Fig. 2(b), the intersection angle of (110) and ($1\bar{1}0$) is 65.16°. Therefore, most newly-grown crystals display a typical rhombus morphology, consistent with the observations shown in Fig. 3. The newly-grown metastable β-HgI$_2$ is similar to the two-dimensional in terms of crystal size, and the layer shape of (111) and (112) faces was therefore difficult to observe (Fig. 3), although their attachment energy is very close to that of (110). The (010) face has the largest attachment energy among the five faces listed in Table 1, which implies the fastest growth rate, and hence instability. This may be the reason why tetragonal or rectangular forms of metastable β-HgI$_2$ are not easy to acquire. Therefore, the growth form of metastable β-HgI$_2$ layer in crystals grown from the solution could be derived from classical PBC theory, and the morphological importance decreases differently in the order {001}>{110}>{111}>{112}>{010}.

Fig. 5. The phase transformation of metastable β-HgI$_2 \rightarrow \alpha$-HgI$_2$

Metastable β-HgI$_2$ is mechanically unstable due to the Van der Waals forces between crystals, as shown in Fig.

2(a). We recorded the phase transformation process using a polarizing microscope at 25°C, as shown in Fig. 5. Four regular crystals were present during the entire period, and were labeled as C1 to C4. Nine photos of the metastable β-HgI$_2$→α-HgI$_2$ phase transformation were captured in 45 s, and the whole recording time was ~ 480 s (Fig. 5).

Metastable β-HgI$_2$ is mechanically unstable due to the Van der Waals forces between crystals, as shown in Fig. 2(a). We recorded the phase transformation process using a polarizing microscope at 25°C, as shown in Fig. 5. Four regular crystals were present during the entire period, and were labeled as C1 to C4. Nine photos of the metastable β-HgI$_2$→α-HgI$_2$ phase transformation were captured in 45 s, and the whole recording time was ~ 480 s (Fig. 5).
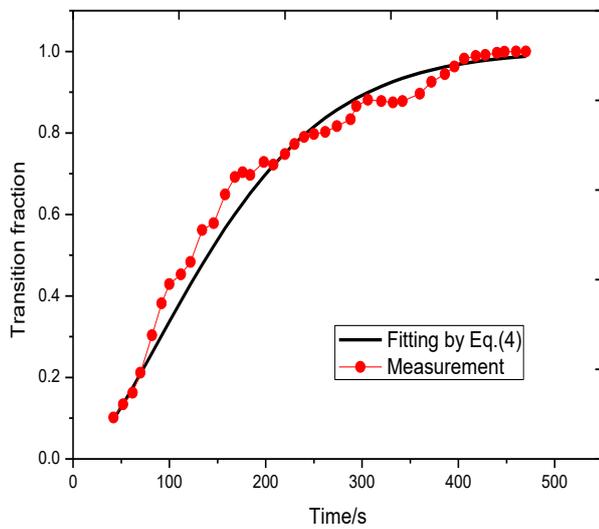

Fig. 6. The dependence of the area fraction and the transformation time plot on the metastable β-HgI$_2$→α-HgI$_2$ phase transformation

As shown in Fig. 5, a tiny red nucleus appeared at the junction of C1 and C2, and propagated around to two crystals at a relatively slow rate. After 150 s, the transformation reached C3, and after 300s, the C4 phase change began. Contours of all crystals were not remarkably altered during the phase change. Because the phase transformation of crystals was similar to the two-dimensional form, the rate of the phase change could be calculated as S/S_0, where S and S_0 are the area of transformed crystals and the initial area of metastable β-HgI$_2$, respectively (based on stereology, $S_a/S_{beta}=V_a/V_{beta}$, where S_a is the area of the transformed phase, S_{beta} is the area of the initial phase, V_a is the volume of the transformed phase, and V_{beta} is the volume of the initial phase. It should be noted that the value of S recorded was the sum of areas in four crystals). The measurement of areas was carried by Image J processing software. The dependence of the transformation time (t) on the ratio (f) was therefore investigated.

Table 1. Interplanar spacing (d_{hkl}) and attachment energy (J/mol) of the main face of metastable β-HgI$_2$

hkl	{001}	{110}	{111}	{010}	{112}
d_{hkl}	6.9715	3.9888	3.8350	3.7041	3.4621
E_{hkl}^{att}	7.55	18.40	18.49	21.69	19.39

The curve of f and t (Fig. 6) was drawn to investigate the correlation between the transformed volume fraction, f, and the transformation time, t, which displayed an approximate "S" shape, corresponding to a typical phase change. According to the Johnson-Mehl-Avrami-Kolmogorov (JMAK) method [32], the relationship between f and t could be expressed as:

$$f = 1 - \exp[-(t/K)^n] \qquad (3)$$

where K is the time constant, and n is the growth exponent. Because the value of n in Eq. (3) is assumed to be constant [33], and the initial transition time is difficult to determine, the start of the transition is t_0, Eq. (3) can be written as:

$$f = 1 - \exp[-((t-t_0)/K)^{n(t)}] \qquad (4)$$

Eq. (4) considers the change in the growth mode over time as a transition fraction. Using Eq. (4), the measured data were fitted as shown in Fig. 6, and the experimental result could be fitted. The fitted parameters are $t_0 = 4.1432$ s, $K = 73.37$ and $n = 1.5$. From the classical JMAK theory, n is an integer dependent on the shape of the growing crystalline body [34]. The value $n=1.5$ indicates that the growth mode is between one-dimensional and two-dimensional growth [35]. In fact, the video appeared to show one-dimensional growth and two-dimensional growth at different times, which indicates that the phase change is a layer-by-layer process from the outside to the inside (i.e. the growth dimension may change from one to two in the metastable β-HgI$_2$→α-HgI$_2$ phase transformation).

The structure of α-HgI$_2$ has a typical almost cubic close-packed substructure composed of iodine atoms at a quarter of the tetrahedral interstices, and all I-Hg-I and Hg-I-Hg angles are close to tetrahedral [28], as shown in Fig. 2(c). Additionally, the metastable β-HgI$_2$ molecule has a linear I-Hg-I structure, as shown in Fig. 2(a). Molecules 1, 2 and 3 in β-crystals were stimulated and diffused over a short distance due to the small change in surroundings and the intermolecular distance. These molecules could then impact each other and form the tetrahedral structure of $[HgI_4]^{2-}$ shown in Fig. 2(c). The iodide ion in molecule 3 of metastable β-HgI$_2$ (I3'') could then bind to mercury ion (Hg1), and I2'' in molecule 2 could also bind to the mercury ion (Hg1) to form the structure of $[HgI_4]^{2-}$. For the HgI$_2$ molecule, 6s and 6p orbital in Hg hybridise to form two linear distributions of I. Meanwhile, four bonds involving Hg-I are formed by sp^3

hybridisation in [HgI$_4$]$^{2-}$, two of which are σ-bonds in Hg-I, and two of which coordinate in Hg-I. Hence, the nature of the $\beta \rightarrow \alpha$ phase change involves diffusion of I$^-$ over a short distance, binding to Hg$^+$ of the neighbouring HgI$_2$ molecule, and formation of [HgI$_4$]$^{2-}$. Obviously, the formation of [HgI$_4$]$^{2-}$ in α-HgI$_2$ requires the formation of chemical bonds [26], which is destructive to the structure, although the shape of the metastable β-HgI$_2$ does not appear to change obviously during the phase transformation.

Based on the results shown in Fig. 5, two phases appear to coexist, and β-HgI$_2$ and α-HgI$_2$ correspond to the parent and product phases, respectively. Consequently, the metastable β-HgI$_2 \rightarrow \alpha$-HgI$_2$ phase transformation is a first-order transition of structure reconstruction. Faster evaporation favours the formation of metastable β-HgI$_2$ [28]. For seed layer growth in solution to prepare iso-epitaxy vapor-grown HgI$_2$ film, slow solvent evaporation would promote higher crystallinity in α-HgI$_2$, and this favours the preferred orientation of polycrystalline α-HgI$_2$.

4. Conclusion

In summary, successive crystal growth phases of metastable β-HgI$_2$ and the metastable β-HgI$_2 \rightarrow \alpha$-HgI$_2$ phase transformation were investigated using polarising microscopy. During growth, the growing crystal appears to form a layered rhombus with a sharp angle of ~65.24°. Most newly-grown crystals appear rhomboid and have a sharp angle of 65.0 ± 0.35°. This is consistent with the included angle of (110) and (1$\bar{1}$0) of 65.16° calculated using Diamond software, and indicates quasi-equilibrium growth. The morphological importance of metastable β-HgI$_2$ decreases differently in the order {001}>{110}>{111}>{112}>{010} according to the attachment energy calculated using MS software based on PBC theory, which indicates the possible morphological character. Using a modified JMAK equation, the experimental results fitted well, giving a growth exponent $n = 1.5$, indicating growth between one-dimensional and two-dimensional growth. The nature of the β-HgI$_2 \rightarrow \alpha$-HgI$_2$ phase transformation involves diffusion of I$^-$ over a short range, binding to Hg$^+$ of a neighbouring HgI$_2$ molecule, and formation of [HgI$_4$]$^{2-}$. This phase transformation belongs to a first-order transition structure reconstruction.

References

[1] M. M. Gospodinov, D. Petrova, I. Y. Yanchev, M. Daviti, M. Manolopoulou, K. M. Paraskevopoulos, A. N. Anagnostopoulos, E. K. Polychroniadis, J. Alloy. Compd. **400**, 249 (2005).

[2] J. T. Tang, D. T. Li, Z. X. Feng, C. Y. Long, J. Alloy. Compd. **653**, 310 (2015).

[3] M. Schieber, A. Zuck, J. Optoelectron. Adv. M. **5**, 1299 (2003).

[4] R. M. Rama, J. K. D. Verma, A. P. Patro, J. Phys. D Appl. Phys. **13**, 1545 (1980).

[5] P. Bohac, J. Cryst. Growth **61**, 163 (1983).

[6] M. N. Jovan, H. Rajna, I. M. Olga, Langmuir **8**, 299 (1992).

[7] L. Fornaro, L. Luchini, M. Köncke, L. Mussio, E. Quagliata, K. Chattopadhyay, A. Burger, J. Cryst. Growth **217**, 263 (2000).

[8] F. Gaizer, G. Johansson, F. Sandberg, T. Norin, F. Gaizer, G. Johansson, F. Sandberg, T. Norin, Acta Chem. Scand. **22**, 3013 (1968).

[9] R. C. Carlston, M. M. Schieber, W. F. Schnepple, R. C. Carlston, M. M. Schieber, W. F. Schnepple, Mater. Res. Bull. **11**, 959 (1976).

[10] I. F. Nicolau, J. Cryst. Growth **48**, 51 (1980).

[11] I. F. Nicolau, J. P. Joly, J. Cryst. Growth **48**, 61 (1980).

[12] W. C. Barber, N. E. Hartsough, J. S. Iwanczyk, IEEE T. Nucl. Sci. **56**, 1012 (2009).

[13] A. Burger, D. Nason, L. Franks, J. Cryst. Growth **379**, 3 (2013).

[14] G. Zentai, M. Schieber, L. Partain, R. Pavlyuchkova, C. Proano, J. Cryst. Growth **275**, e13271 (2005).

[15] M. Schieber, H. Hermon, A. Zuck, A. Vilensky, L. Melekhov, R. Shatunovsky, E. Meerson, Y. Saado, M. Lukach, E. Pinkhasy, S. E. Ready, R. A. Street, J. Cryst. Growth **225**, 118 (2001).

[16] B. E. Patt, N. Skinner, Proc. SPIE **4508**, 28 (2001).

[17] H. B. Barber, H. Roehrig, F. P. Doty, R. C. Schirato, E. J. Morton, Proc. SPIE **4508**, 119 (2001).

[18] A. L. Noguera, M. E. Pérez, E. Quagliata, L. R. Fornaro, J. Cryst. Growth **310**, 1691 (2008).

[19] C. T. Shih, T. J. Huang, Y. Z. Luo, S. M. Lan, K. C. Chiu, J. Cryst. Growth **280**, 442 (2005).

[20] M. Schieber, A. Zuck, H. Gilboa, G. Zentai, IEEE T. Nucl. Sci. **53**, 2385 (2006).

[21] A. Zuck, M. Schieber, O. Khakhan, H. Gilboa, Z. Burshtein, IEEE T. Nucl. Sci. **21**, 1250 (2004).

[22] L. Fornaro, I. Aguiar, M. E. Pérez, H. B. Pereira, IEEE Nuclear Science Symposium conference record. Nuclear Science Symposium **612**, 3923 (2010).

[23] L. Fornaro, I. Aguiar, M. E. Pérez, A. Olivera, I. Galain, M. Mombrú, J. Cryst. Growth **401**, 489 (2014).

[24] L. Fornaro, J. Cryst. Growth **379**, 115 (2013).

[25] M. Hostettler, H. Birkedalt, D. Schwarzenbach, Helv. Chim. Acta **86**(5), 1410 (2003).

[26] M. Hostettler, H. Birkedalt, D. Schwarzenbach, Acta.

Crystallogr. Sect. B: Struct. Sci. **B58**, 903 (2002).

[27] M. Hostettler, D. Schwarzenbach, C. R. Chim. **8**(2), 147 (2005).

[28] J. W. Cahn, Acta Metallurgica **4**, 572 (1956).

[29] I. K. Akopyan, M. É. Labzovskaya, B. V. Novikov, V. M. Smirnov, Phys. Solid State **49**, 1375 (2007).

[30] P. Hartman, W. G. Perdok, Acta Crystallogr. **8**, 521 (1955).

[31] P. Hartman, P. Bennema, J. Cryst. Growth **49**, 145 (1980).

[32] D. Kashchiev, Nucleation: Basic Theory and Applications, Butterworth-Heinemann, Oxford, (2000).

[33] K. Sangwal, Additives and Crystallization Processes: From Fundamentals to Applications, Wiley, Chicheser, (2007).

[34] I. H. Hillier, J. Polym. Sci. **A3**, 3067 (1965).

[35] J. W. Christian, The Theory of Transfomation in Metals and Alloys, Part 1 Equilibrium and General Kinetics Theory, Oxford, Pergamon Press, 1975.

[*]Corresponding authors: xxrshhuangshan@126.com